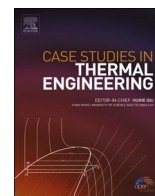


Contents lists available at [ScienceDirect](https://www.sciencedirect.com)

Case Studies in Thermal Engineering

journal homepage: www.elsevier.com/locate/csite

Demonstrating the significance of radiant energy exchange during metal dust combustion

Harrison Jones^a, Pascal Dube^a, Quan Tran^b, Michelle L. Pantoya^{b,*}, Igor Altman^{c,**}

^a Matsys, Inc., Sterling, VA, 20164, USA

^b Department of Mechanical Engineering, Texas Tech University, Lubbock, TX, 79424, USA

^c Combustion Sciences and Propulsion Research Branch, Naval Air Warfare Center Weapons Division, China Lake, CA, 93555, USA

ARTICLE INFO

Handling Editor: Huihe Qiu

Keywords:

Aluminum particle combustion
Metal powder suspension
Bomb calorimetry
Heat balance
Radiative loss

ABSTRACT

Metal combustion is a process accompanied by strong light emission. Correspondingly, radiative loss can significantly affect the overall energy balance, and needs to be considered in the global numerical models describing metal dust combustion. In this work, we experimentally estimated the fraction of radiative loss during aluminum (Al) dust combustion by studying the heat release in a modified constant volume bomb calorimeter that enabled the additional measurement of pressure. The previously developed method of dispersing powder ensured nearly 100% combustion efficiency. The contribution of the combustion energy to heating the gas inside the calorimeter bomb was determined by analyzing the measured pressure traces and found to be measurably lower than 100%. The energy loss was attributed to radiant heat transfer from burning metal particles to the bomb wall. Aluminum powders with median size ranging from 4 μm to 100 μm were studied. The estimated fraction of radiative loss depended on the particle size. Radiative loss saturated at nearly 50% for larger particles and gradually reduced with the particle size decrease below 20 μm . We related the observed radiative loss to a recently introduced process that occurs during metal combustion, namely condense-luminescence. The results shown here have important implications for the role of radiant energy exchange in metal particle combustion and will transform future approaches to harnessing metal oxidation energy for a multitude of applications.

1. Introduction

Metal-based reactive materials have great potential for energetic applications such as propellants and explosive systems [1,2]. Comprehending the role of radiant energy transfer in the overall heat balance of metal oxidation reactions is important for the description of flame propagation in metal suspensions [3] as well as modeling the global energy exchange process [4]. Despite decades of study (since 1950s), puzzles continue to limit the current understanding of metal combustion. Historically, the challenges were partly caused by adapting models of hydrocarbon droplet combustion to describe inorganic solid materials, despite their inherently different chemical and physical properties [5].

One of the major differences between hydrocarbon and metal combustion is related to the final combustion products. Gases such as CO_2 , H_2O are produced in the case of hydrocarbon combustion in an oxygen-rich environment, while condensed oxide nanoparticles

* Corresponding author;

** Corresponding author.

E-mail addresses: michelle.pantoya@ttu.edu (M.L. Pantoya), igor.altman2.civ@us.navy.mil (I. Altman).

<https://doi.org/10.1016/j.csite.2023.102809>

Received 19 December 2022; Received in revised form 1 February 2023; Accepted 8 February 2023

Available online 10 February 2023

2214-157X/© 2023 The Authors. Published by Elsevier Ltd. This is an open access article under the CC BY-NC-ND license (<http://creativecommons.org/licenses/by-nc-nd/4.0/>).

are formed from metal combustion. Unlike hydrocarbons, metal flames produce broad light emission originating from condensed species. High radiative loss in metal-containing flames is related to the mechanism of light emission from the condensing nano-oxide species generated during metal combustion. Radiation loss from formation of nano-oxides is a major channel for dissipating energy released upon condensation and coined condense-luminescence [5,6]. Radiative loss associated with this light emission also makes the system non-adiabatic, an issue commonly ignored. However, quantifying radiative loss accurately is crucial, in particular for either justifying or invalidating the adiabatic assumption common in current models of metal combustion.

There is limited literature on direct measurements of the absolute value of radiative loss in metal flames. One experiment was carried out with a single burning magnesium (Mg) particle, and radiative loss of about 40% of the total heat of combustion was reported independent of the varied metal particle size [7]. Extending single particle measurements to dust clouds or particle suspensions should be done for more precise characterization of energy exchange processes.

The objective of this investigation was to quantify radiative loss during aluminum (Al) powder combustion within a modified constant volume bomb calorimeter designed to enable pressure measurements. The experiment was designed as an alternative to steady-state metal dust flames coupled with a bolometer that is capable of measuring radiation in the entire spectral range. In the modified bomb calorimeter, coupling pressure measurements with calorific output from Al powder oxidation ensured that metal powder combustion was complete. Then, the observed pressure underperformance can be attributed to radiative loss.

It is noted that constant volume combustion chambers are commonly used to investigate metal oxidation. Results often show that the pressure peaks are lower than theoretical predictions [8,9]. Previous research using constant volume chambers did not simultaneously allow for calorific output measurements, such that reduced pressures were attributed to combustion quenching by the chamber walls rather than to the non-adiabatic system behavior caused by substantial radiation exchange. The diagnostic used to accomplish the objective here was purposefully designed to ensure complete combustion while measuring transient pressure and mitigate issues associated with data analysis resulting from quenched or unreacted metal powder.

2. Experimental

A Parr 6100 Compensated Jacket Calorimeter (Parr Instrument Co.) was utilized for measuring the calorific output of burning metal powders as described in our previous work [6,10]. The corresponding calorimetry experiments were required to ensure metal combustion completeness that is essential for further interpretation of the pressure measurements. Separately, the oxygen bomb component of the calorimeter was modified by adding a pressure transducer connected to a Parr 6796 Dynamic Pressure Recording, which allowed for recording the temporal pressure evolution during combustion. The modification did not affect the available bomb volume of 240 ml. All combustion experiments were performed under oxygen atmosphere at the pressure of 400 psi.

Aluminum powders supplied by Valimet, Inc. with six characteristic metal particle diameters of 3.5 μm , 8 μm , 12 μm , 31 μm , 55 μm and 108 μm (Valimet Product No. H-2, H-5, H-10, H-30, H-50 and H-95, respectively) [11] were used in experiments. In order to suspend the metal powder in the bomb, the powders were dispersed in a porous medium that is a starch-based material composed of poly-carbohydrates, including corn and potato starches. This porous poly-carbohydrate (PP) microstructure was previously demonstrated to provide a readily combustible hydrocarbon medium to disperse the powder and simulate metal powder suspensions [6,10]. In experiments, the nominal mass of dispersing material was 0.0295 g and the nominal mass of metal powder was 0.0395 g. At these nominal masses, the heat of metal combustion is about 2.5x the heat of PP combustion and thereby minimizes possible interference of the spiking agent. The latter does not look avoidable if alcohols are used. The coarse Al powder (H-30, H-50 and H-95) samples of the triple nominal mass (0.1185 g) were also tested. Separately, the pure PP samples of varied masses (1x – 4x the nominal mass) were tested to obtain the instrument operational curves for data analytics as further defined below.

3. Data processing approach

The purpose of the current study was to experimentally quantify the metal energy contribution to the system pressure during combustion, and, correspondingly, to infer the lost (non-contributing) energy that can be attributed to radiative loss. Commonly, in constant volume combustion experiments [8,9], the measured peak pressure is compared to the thermodynamically based expected value. Then, assuming adiabatic system behavior the pressure underperformance is attributed to incomplete metal combustion. Our auxiliary calorimetry tests demonstrated metal calorific output nearly 100% of its theoretical value and led to a need to reconsider assumptions of incomplete combustion in the adiabatic system as an explanation of lower pressures. Thus, experimental results showed the necessity to consider the non-adiabatic system and quantify energy losses responsible for the observed pressure anomaly during combustion of metal suspensions.

Conduction, convection, and radiation contribute to energy exchange within the bomb during combustion resulting in the overall measured calorific output. At the same time, conduction and convection, which originate from the gas heating, appear due to the direct contribution of combustion energy to heat, and, therefore, to pressure. Conduction and convection heat the gas environment within the bomb registering a pressure differential. The radiation-related energy exchange does not affect the gas pressure. Radiation is exchanged with the bomb wall instead. Then, studying pressure characteristics allows for isolating radiation loss and quantifying its fraction in the overall energy balance. In the overall energy balance of the calorimeter, the contribution of radiant exchange can be partitioned from gaseous heating resulting from conduction and convection. It should be added that in the case of burning Al particles colliding with the bomb wall, their combustion would be quenched resulting in reduced calorific output. Thus, the combustion completeness confirmed in the auxiliary tests allowed exclusion of the interface heat exchange on the bomb wall from the energy balance consideration.

For data analytics, our approach directly quantifies the metal energy that contributes to the measured pressure. The analysis begins

with the recorded pressure characteristics for different amounts of burning PP samples. Then, the dependence of that pressure characteristic on the energy of the PP sample was considered the instrument operational curve. The corresponding measured pressure characteristic resulting from combustion of the metal powder in the PP allowed quantifying the metal energy that contributed to the system pressurization. The latter assumed equivalency of the contributing metal and PP energies into the pressure. The inferred equivalent contributing metal energy was lower than the available (calorific) energy of the material. The difference was interpreted as additional energy loss that is present in the metal-containing burning suspensions compared to the PP.

Two pressure characteristics of burning systems were considered. The first was the maximum (peak) pressure achieved during combustion. The second was the integral under the time-dependent pressure curve, and its relevance is justified below.

Based on the Gay-Lussac's gas law, the pressure, P , and temperature, T , of the gas within the constant volume system are related to their initial values, P_0 and T_0 as

$$\frac{P}{P_0} = \frac{T}{T_0}. \quad (1)$$

Then, the overpressure measured by the transducer, $\Delta P \equiv (P - P_0)$, is proportional to the gas overheating $\Delta T \equiv (T - T_0)$, and $\Delta T \propto \Delta P$. On the other hand, the heat flux from the gas to the bomb wall, J , is also proportional to the gas overheating, i.e., $J \propto \Delta T$. Thus, the overall heat transferred from the system to the wall by conductive and convective heat transfer, Q^{tr} , is related to the overpressure integral over time (the area under the measured pressure curve) as $Q^{tr} \equiv \int_0^\infty J(t) dt \propto \int_0^\infty \Delta P(t) dt$. This transferred energy is equal to the overall heat released within the bomb. Therefore, the integral $\int_0^\infty \Delta P(t) dt$ is a representative characteristic of the system behavior.

A typical pressure trace and peak pressure and area metrics used in the data analysis are shown in Fig. 1.

An operational curve generated by plotting the peak pressure, which resulted from burning the 1x – 4x nominal mass PP samples as a function of the fuel energy, is shown in Fig. 2. The fuel energy (the X-axis) is calculated as a product of the PP sample mass and the PP heat of combustion $\Delta H_{PP} = 16.61$ kJ/g [10].

In Fig. 2, also sketched is the contributing metal energy, Q_{Al}^{ctr} , and the lost Q_{Al}^{lst} metal energy that are determined using the measured peak pressure resulting from the PP + metal sample combustion. The available metal energy, Q_{Al}^{avl} , is calculated as a product of the metal powder mass and the aluminum heat of combustion $\Delta H_{Al} = 31.05$ kJ/g [12]. The corresponding data analysis approach based on the integral $\int_0^\infty \Delta P(t) dt$ (shaded area in Fig. 1) is exactly the same and uses the operational curve generated from the overpressure integral, which is shown as the inset in Fig. 2.

Attributing the lost energy to radiant exchange and considering complete metal combustion, the fraction of radiative loss can be calculated using Eq. (2).

$$R_{\%} \equiv \frac{Q_{Al}^{lst}}{Q_{Al}^{avl}} \cdot 100\% = \frac{Q_{Al}^{avl} - Q_{Al}^{ctr}}{Q_{Al}^{avl}} \cdot 100\% \quad (2)$$

In Eq. (2) the available metal energy, Q_{Al}^{avl} is calculated based on the metal powder mass. The contributing metal energy, Q_{Al}^{ctr} , is obtained from the corresponding peak- or area-based analysis.

4. Results and discussion

Experimentally estimated radiative losses during combustion of different Al powders are presented in Fig. 3. All data were obtained from either the peak pressure or the area under the pressure trace as detailed in the previous section.

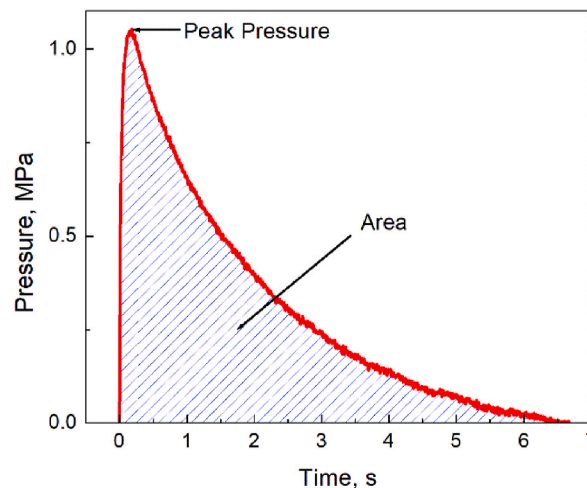


Fig. 1. The typical pressure trace and characteristics used in the data analysis.

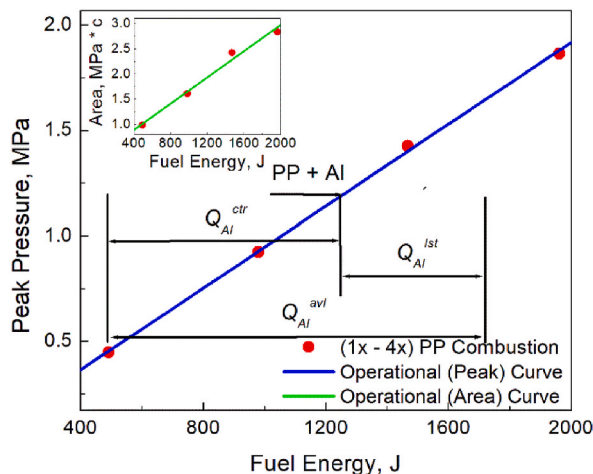


Fig. 2. Operational curve that relates peak pressure with the fuel energy. The inset shows the operational curve that relates the area under the pressure trace with the fuel energy. Both operational curves result from burning the PP of 1x - 4x the nominal mass. The equivalency approach to quantify the contributing metal energy during the PP + metal sample combustion is also sketched. The approach works in the same way regardless of which operational curve is processed. In the sketch, the available metal energy is Q_{Al}^{avl} , the contributing metal energy to heat in the gas is Q_{Al}^{ctr} , and the lost metal energy is Q_{Al}^{lst} . The equivalent contributing metal energy is the difference between the abscissa of the point on the operational curve corresponding to the pressure characteristic achieved by burning the PP + Al sample and the energy of the pure PP of the nominal mass.

The radiative losses estimated from the pressure peak data provide an upper bound. The reason for the variation between peak and area analysis is related to a time delay between ignition and pressure peaking which results in an upper limit for radiative loss. Corresponding conductive and convective loss originating from heat transfer to the bomb wall are included in radiative loss calculations using the operational curve based on the peak pressure.

The approach using the operational curve based on area under the pressure trace directly provides the overall heat that is transferred from the gas to the wall. Thus, estimating the metal energy that contributes to heating the gas and inferring radiative loss from the area data is a more accurate procedure. Processing the peak pressure data along with the area data (as presented in Fig. 3) highlights differences in accuracy. It also illustrates the magnitude of overestimate of radiative loss if it is inferred from the peak pressure data rather than from the overpressure integral.

We were not able to clearly conclude whether the radiative loss scatter in Fig. 3 is a result of error accumulations during data processing or originates from test-to-test variations. At the same time, incomplete combustion, if any, cannot significantly lower the reported loss values (see a discussion below). The trend in radiative loss shown in Fig. 3 is real and nearly flat for large particles and gradually reduces as particle size decreases below 20 μm . Note that the noticeable change in the trend occurs at about the same particle size that particle burn time dependence on the particle diameter has the well-known knee inflection [13]. This knee is commonly

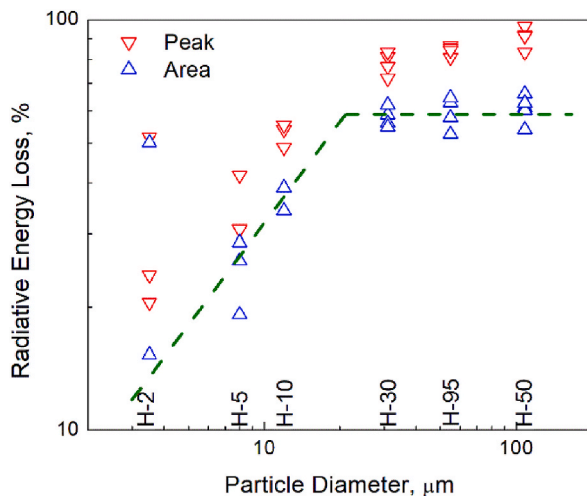


Fig. 3. The radiant energy losses estimated from the operational curves using either "Peak" or "Area" pressure characteristics as a function of Al particle size. The manufacturer's powder names are included for clarity. The dashed (Green) line shows the major trend and is provided as a guide for visualization. (For interpretation of the references to colour in this figure legend, the reader is referred to the Web version of this article.)

considered a boundary between different regimes of Al particle combustion (i.e., volumetric compared to surface-occurring).

In order to understand the trend in radiative loss and the significance of radiation fraction in the overall energy balance, the origin of light emission during metal combustion should be analyzed. It had been explained [14] that the anomaly related to optical pyrometry in metal flames appears due to the strong radiation from nano-oxides formed as a result of metal combustion. Emission characteristics of nano-oxides depend on peculiarities of their formation by condensation. Recently, the combustion community has arrived at a consensus on the essential role of light emission from formed nano-oxides in measured flame spectra [15]. Then, a variation in the radiative loss magnitude seen in Fig. 3 is likely related to the change of light emission from generated nano-oxides and has nothing to do with radiation from burning metal particles. The metal particles burn at about the same temperature regardless of their size, and therefore, should have same irradiances. Light emission from nano-oxides formed during metal combustion is of the condense-luminescent nature [5,6]. That radiation is an essential condition of nanoparticle formation and is the major channel of dissipating the condensation energy which is on the order of 5 eV per condensing molecule. Thus, the magnitude of radiation emitted by nano-oxides is related to the condensation mechanism (specifically, to the value of energy released during the process) rather than to the nanoparticle temperature.

As explained in Ref. [16], the knee between the different burn time dependencies is also the boundary between different regimes of conductive heat transfer for burning particles. Based on that change in conductive heat transfer regimes, it is possible to address the energy balance paradox for small burning particles [16,17]. Then, depending on the burning particle size, the gas temperature around the particle is substantially different and can significantly affect the condensation regime of gaseous aluminum suboxides forming condensed nano-oxides. Also, large Al particles burn in the vapor-phase regime with AlO being the major gaseous suboxide. For small burning Al particles, Al₂O formed via semi-heterogeneous combustion [5] becomes dominant. The differences in reaction pathways lead to different possible mechanisms of condensation that have different energies. Therefore, formation of nano-oxides that involve the AlO route, the gaseous suboxide with a higher enthalpy [12], would ultimately generate greater radiation compared to the Al₂O route. Then, the radiant energy loss trend seen in Fig. 3 can be qualitatively explained. The comprehensive discussion of that trend is beyond the scope of the current study that experimentally isolated the phenomenon.

In the case of incomplete metal combustion, the available metal energy, Q_{Al}^{avl} in Eq. (2), becomes $\eta \cdot Q_{Al}^{avl}$, with η being the percent of combustion completeness. Then, radiative loss calculated using Eq. (2) would be overestimated according to Eq. (3).

$$\Delta R_{\%} = (100\% - R_{\%}) \cdot \left(\frac{100\%}{\eta} - 1 \right). \quad (3)$$

At radiative losses, $R_{\%}$, of 50–60% obtained for large particles and combustion completeness of about 90%, the overestimate, $\Delta R_{\%}$, described by Eq. (3) and the corresponding lowering of the saturated trend shown in Fig. 3 would be about 5%. This error analysis still leaves radiative loss substantial (i.e., $\geq 50\%$) for all large particle sizes. The overestimate for small particles is more sensitive to the combustion completeness due to smaller absolute values of radiative losses, and, therefore, due to larger values of the factor $(100\% - R_{\%})$ in Eq. (3). As a result, combustion incompleteness would lead to a slightly steeper trend compared to that presented in Fig. 3 for small particles.

The auxiliary experiments on the metal calorific output confirm that the combustion completeness under conditions used for pressure measurements was close to 100% in the majority of tests, with the lowest limit of 90% as summarized in Table 1. The error in Table 1 validates the general conclusions on the radiative loss trend described above and confirms the significance of radiative loss in the total energy balance.

5. Concluding remarks

The experimental quantification of radiative losses during combustion of Al powder suspensions performed in the current study demonstrates the significance of radiation in the heat balance. Radiation exchange makes the system essentially non-adiabatic and must be considered in global numerical models describing the energy exchange process.

Radiative losses exhibit a nearly flat, saturated behavior for large particles and a gradual reduction with particle size decrease for small particles. We relate the revealed trend to regimes of metal particle combustion (volumetric vs. surface-occurring) that are widely understood for describing particle burn time trends as a function of particle size. Peculiarities of heat transfer between the burning particle and environment, which depend on volumetric vs. surface-occurring combustion regimes, affect conditions of nano-oxide formation that is the process responsible for light-emission and influence radiant exchange.

Attributing radiative loss to light emission from nano-oxides formed during metal powder combustion explains the high values (i.e., $\geq 50\%$) of radiation in the energy balance. Radiant emission is based on the condense-luminescent nature of the process that is an essential mechanism of dissipating the energy released during nano-oxide growth.

Author credit statement

Harrison Jones: Investigation, Methodology, Data curation, Pascal Dube: Conceptualization, Methodology, Supervision, Quan Tran: Methodology, Validation, Michelle Pantoya: Writing – review & editing, Supervision, Project administration, Funding acquisition, Igor Altman: Conceptualization, Formal analysis, Investigation, Writing – original draft.

Declaration of competing interest

The authors declare that they have no known competing financial interests or personal relationships that could have appeared to

Table 1

The completeness of metal combustion for different tested Al powders calculated as a ratio of the measured calorific output to the handbook value. The error is experimental scatter.

Al Powder	H-2	H-5	H-10	H-30	H-50	H-95
Completeness, %	97.7	92.5	95.6	95.5	97.1	90.4
Error, %	5.2	2.2	5.1	3.6	3.1	2.8

influence the work reported in this paper.

Data availability

Data will be made available on request.

Acknowledgements

HJ and PD acknowledge support from the Army's Combat Capabilities Development Command Armaments Center under contract DOTC 19-01-INIT0157 for the development of novel analytical capabilities for reactive materials. The authors from TTU (QT, MP) are grateful for support from United States Office of Naval Research (ONR) grant number N00014-22-2006 and Dr. Chad Stoltz and ONR STEM grant N00014-21-2519 and Dr. Michael Simpson. Also, IA is thankful for funding from the NAVAIR ILIR program managed at the ONR and administered by Dr. Alan Van Nevel.

References

- [1] E.W. Price, R.K. Sigman, Combustion of aluminized solid propellants, in: V. Yang, T.B. Brill, W.Z. Ren (Eds.), *Solid Propellant Chemistry, Combustion, and Motor Ballistics*, AIAA, New York, 2000, pp. 663–687.
- [2] D. Sundaram, V. Yang, R. Yetter, Metal-based nanoenergetic materials: synthesis, properties, and applications, *Prog. Energy Combust. Sci.* 61 (2017) 293–365.
- [3] S. Goroshin, J. Palečka, J.M. Berghorson, Some fundamental aspects of laminar flames in nonvolatile solid fuel suspensions, *Prog. Energy Combust. Sci.* 91 (2022), 100994.
- [4] M. Beckstead, Y. Liang, K. Pudduppakkam, Numerical simulation of single aluminum particle combustion (Review), *Combust. Explos. Shock Waves* 41 (2005) 622–638.
- [5] I. Altman, M. Pantoya, Comprehending metal particle combustion: a path forward, propellants, explosives, *Pyrotechnics* 47 (2022), e202200040.
- [6] Q. Tran, M.L. Pantoya, I. Altman, Condense-luminescence and global characterization of metal particle suspension combustion, *Appl. Energy Combust. Sci.* 11 (2022), 100080.
- [7] Y. Shoshin, I. Altman, Integral radiation energy loss during single Mg particle combustion, *Combust. Sci. Technol.* 174 (2002) 209–219.
- [8] P.R. Santhanam, V.K. Hoffmann, M.A. Trunov, E.L. Dreizin, Characteristics of aluminum combustion obtained from constant-volume explosion experiments, *Combust. Sci. Technol.* 182 (2010) 904–921.
- [9] R. Lomba, S. Bernard, P. Gillard, C. Mounaïm-Rousselle, F. Halter, C. Chauveau, T. Tahtouh, O. Guézet, Comparison of combustion characteristics of magnesium and aluminum powders, *Combust. Sci. Technol.* 188 (2016) 1857–1877.
- [10] Q. Tran, I. Altman, P. Dube, M. Malkoun, R. Sadangi, R. Koch, M.L. Pantoya, Direct demonstration of complete combustion of gas-suspended powder metal fuel using bomb calorimetry, *Meas. Sci. Technol.* 33 (2022), 047002.
- [11] Valimet Inc, Chemical and physical characteristics of valimet aluminum powder specifications, Dataset (available at: <https://valimet.com/wp-content/uploads/2021/08/Aluminum-H-Series-Data-Sheet-.pdf>). (Accessed 1 December 2022). Accessed.
- [12] NIST chemistry WebBook, available at: 2023 <https://webbook.nist.gov> (retrieved 31 January,).
- [13] D.S. Sundaram, P. Puri, V. Yang, A general theory of ignition and combustion of nano- and micron-sized aluminum particles, *Combust. Flame* 169 (2016) 94–109.
- [14] I.S. Altman, Determination of particle temperature from emission spectra, *Combust. Explos. Shock Waves* 40 (2004) 67–69.
- [15] F. Peng, H. Liu, W. Cai, Combustion diagnostics of metal particles: a review, *Meas. Sci. Technol.* 34 (2023), 042002.
- [16] I. Altman, A. Demko, K. Hill, M. Pantoya, On the possible coexistence of two different regimes of metal particle combustion, *Combust. Flame* 221 (2020) 416–419.
- [17] I. Altman, On energy accommodation coefficient of gas molecules on metal surface at high temperatures, *Surf. Sci.* 698 (2020), 121609.